Extended Abstracts of the 2012 International Conference on Solid State Devices and Materials, Kyoto, 2012, pp444-445

PS-13-15

Correlation between electronic properties and structural characteristics of patterned nanographene

Gemma Rius[1], Marc Sansa[2], Xevi Borrise[3], Francesc Perez-Murano[2], Masamichi Yoshimura[4], Osamu Eryu[1], Narcis Mestres[5]

[1]Nagoya Institute of Technology, Gokiso-cho, Showa-ku, 466-8555 Nagoya (Japan)
Phone: +81 52 735 5909 E-mail: rius.gemma@nitech.ac.jp
[2]Institut de Microelectronica de Barcelona-CSIC, Campus UAB, 08193 Bellaterra (Spain)
[3]Institut Catala de Nanotecnologia, Campus UAB, 08193 Bellaterra (Spain)
[4]Toyota Technological Institute, 2-12-1 Hisakata, Tempaku-ku, 468-8511 Nagoya (Japan)
[5]Institut de Ciencia dels Materials de Barcelona, Campus UAB, 08193 Bellaterra (Spain)

1. Introduction

Current processes for the production of high quality and large scale synthesis of graphene are commonly based on the chemical vapor deposition technique. However, these approaches still present serious limitations for a controlled mass production of devices. Efforts to enable their exploitation and finer tuning of specifications have promoted the development of other synthesis processes such as irradiation mediated techniques for the growth of graphene on metals substrates, and the Si sublimation of SiC surface [1].

From a technological point of view, the need to post-process or transfer to suitable substrates is undesirable. Additionally, the evaluation of alternative carbon sources is interesting, as it is the study of the mechanisms for their transformation into desired crystalline nanocarbon materials. Strictly-2D (single layer) graphene is rarely pristine since contains a number of impurities, C or foreign adatoms, vacancies, etc. in addition to the finite crystalline size and support related effects such as conformality, wrinkles and so on. In multilayered graphene these non-idealities are increasingly present, including stacking order and peak shifts and broadening in Raman spectroscopy [2].

For a group of potential applications, the presence of those defects provides interesting properties related to the spin phenomena, for advanced nanoelectronics and to make possible the attachment of specific molecules. Multiple types of graphene nanostructured materials are a real necessity. Knowledge on their electronic, mechanical, etc. properties assesses their potential for applications.

2. Synthesis Methodology

We present a route for the simple and direct fabrication of position, pattern and thickness-controlled nanographene features onto insulating substrates [3]. The preparation of the nanographene in this study is based on, i) the deposition of thickness-controlled amorphous carbon (a-C) patterns by focused ion beam induced deposition (FIBID) on a flat insulator surface (SiO_2) and, ii) the thermal annealing in a vacuum, using a thin metal foil as the catalyst material for the crystallization of the C deposits (as schematized in Fig. 1). This two-steps approach provides desired graphene-like features on selected places of the substrate.

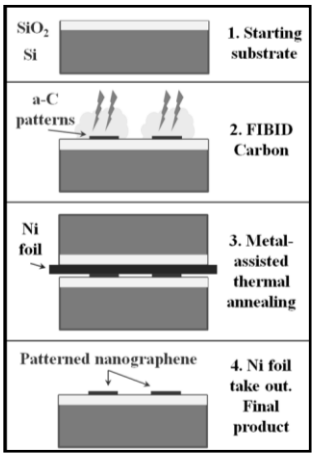

Fig. 1 Schematic illustration of the two-steps process for the site-controlled synthesis of nanographene on SiO_2.

The gallium focused ion beam is operated at 30 kV and with a beam current of 300 pA for the local and controlled deposition of carbon from a gas precursor (*phenanthrene* molecules). The 3D-controlled patterning results from the ion beam induced molecule rupture and momentum transfer, and proper deposition time determines the consequent layer thickness. The present results are based on patterns of 40x40 μm^2 and 40x10 μm^2, and include thicknesses ranging from 5-100 nm. The heating consists of 30 minutes at 975-1000°C, using a lamp furnace operated below 0.4 Pa. The metal catalysts are high purity Ni foils. For the thermal treatment, the patterned chip is covered with a thin Ni foil piece and capped with another SiO_2 on Si chip to promote foil flattening and prevent its movement during pumping. Slight manual pressure during the samples placement tends to increase the presence of metal inclusions incorporated into the patterns. However, after the heating process the Ni foil and capping chip are easily separated since they do not become fused, not being necessary to use metal etching to detach them.

Raman spectra are acquired using the 532 nm laser excitation wavelength. Typical Raman spectra measured after annealing at 1000 °C for patterned areas with deposited a-C thicknesses of 25, 50 and 100 nm are shown in Fig. 2. The typical Raman signatures of graphene are observed at

~1350 cm^{-1} (D-band), ~1590 cm^{-1} (G-band), and ~2695 cm^{-1} (2D-band). In addition, a small shoulder in the G-band is observed at ~1620 cm^{-1} assigned to the D'-band, and the D+D' band centered at 2950 cm^{-1}, which are related to disorder [4]. The I(D)/I(G) ratio has been used to estimate the degree of graphitization (or crystalline size of graphene), assuming that the main source of disorder is related to the graphene edges. The I(D)/I(G) intensity ratio corresponds to a crystallite in-plane size (La) of about 20 nm or smaller. A degree of graphitization inversely proportional to thickness suggests that there is a strong correlation of rate and, probably, an in-depth limiting factor for metal-assisted crystallization using the foil-based method. The similarity of previously reported results indicates that our C-based nanostructures can be identified as nanosized crystalline graphene and they might be partially surrounded by graphitic C. We have tested the same annealing conditions without the Ni foils, confirming that Ni boosts the formation of graphene crystals.

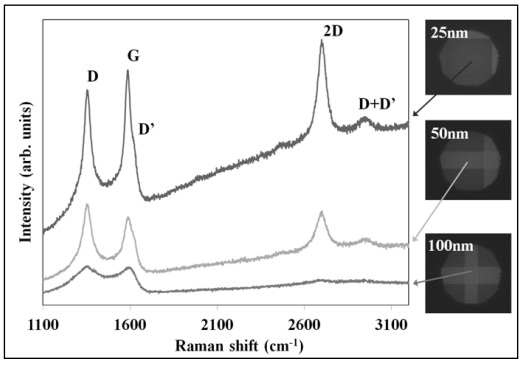

Fig. 2 Raman spectra of 25 nm (top), 50 nm (middle) and 100 nm (bottom) thick C features after annealing at 1000 °C / 30 minutes. Insets are optical microscope images of the patterned areas.

3. Electronic Properties

For the evaluation of the conduction properties of the nanographene patterns, the definition of metal contacts for electrical testing is based on electron beam lithography (EBL). In particular (Fig. 3), (a) Van der Pauw, and (b) (Two) Four Point Probe techniques can be easily implemented thanks to the intrinsic patterning capability of the present synthesis methodology, that is, starting from the FIBID of a-C features.

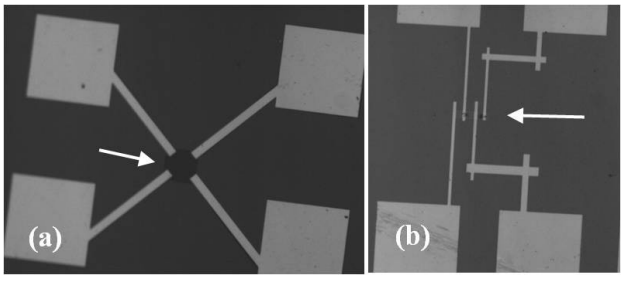

Fig. 3 Optical images of two patterns contacted by EBL. (a) Van der Pauw configuration for a 10 nm thick nanographene and (b) Four-Point Probe configuration of 20 nm thick nanographene.

We analyze the dependence of resistance and anisotropy as a function of nanographene thickness and shape. An example of conduction determined using the Four-Point Probe method is displayed in Fig. 4. The measured resistances are in the order of the kΩ, which is in agreement with the resistivity values for graphite. This can be attributed to the multilayered structure of the nanographene obtained with the present route [3] and also may relate with the finite crystal size, as determined by Raman spectroscopy. Interestingly, the resistivity of nanographene patterns shows certain dependence with the material thickness inversely. We understand this behavior as a weighed and interplayed contribution of several structural aspects of the nanographene pattern structure. In particular, the presence of impurities, the metal-catalyzed degree and anisotropy of graphitization, the amount and arrangement of graphene multilayer, together with the size and continuity of crystalline portions.

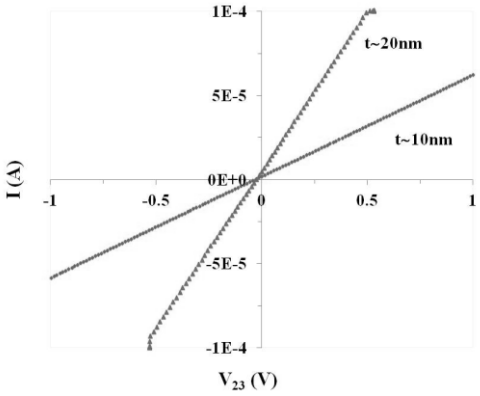

Fig. 4 Electrical characteristics (I/V) of two nanographene devices. Resistances are 5 kΩ for 20 nm thick nanographene and 16.5 kΩ for the 10 nm thick one.

4. Conclusions

We have investigated the electrical conduction properties of site-specific ultrathin nanographene patterns synthesized directly on SiO_2 by FIBID of C and Ni-assisted thermal annealing. The nanographene material shows good electrical conduction and behavior correlated to their structural characteristics and purity. The inclusions consisting of ferromagnetic material and the possibility of performing Van der Pauw technique enable exploration of spintronics phenomena or fundamental analysis such as the evaluation of Hall resistance.

Acknowledgements

We wish to thank the GICSERV access program for granting access to the ICTS CNM Clean room.

References

[1] C. Soldano *et al*, Carbon **48** (2010) 2127–2150.

[2] M. Batzill, Surface Science Reports **67** (2012) 83–115.

[3] G. Rius *et al.* J. of Vac. Sci. Technol. B **30** (2012) 03D113-1.

[4] M. A. Pimenta *et al.* Phys. Chem. Chem. Phys. **9** (2007) 1276.